EPJ Web of Conferences **75**, 01001 (2014)
DOI: 10.1051/epjconf/ 201475 01001

Inter-grain tunnelling in the half-metallic double-perovskites $Sr_2BB'O_6$ (BB'= FeMo, FeRe, CrMo, CrW, CrRe)

B.Fisher,[a] J. Genossar, K. B. Chashka, L. Patlagan and G. M. Reisner

Physics Department, Technion, Haifa, 32000, Israel

Abstract. The zero-field conductivities (σ) of polycrystalline title materials, are governed by inter-grain transport. In the majority of cases their σ(T) can be described by the "fluctuation induced tunnelling" model. Analysis of the results in terms of this model reveals two remarkable features: 1. For *all* Sr_2FeMoO_6 samples of various microstructures, the tunnelling constant (barrier width × inverse decay-length of the wave-function) is ~ 2, indicating the existence of an intrinsic insulating boundary layer with a well-defined electronic (and magnetic) structure. 2. The tunnelling constant for *all* cold-pressed samples decreases linearly with increasing magnetic-moment/formula-unit.

1 Introduction

Half-metallic ordered double-perovskites with fully polarized conduction bands and Curie temperatures (T_c) above room temperature (RT) are of interest for devices which depend on spin polarized transport. Therefore their magnetic, electronic and in particular their magneto-resistive properties [1] have been investigated intensively over the past two decades. The grain boundaries in these materials act in most cases as tunnel barriers. The early theories of inter-grain magneto-resistance due to tunnelling through a non-magnetic barrier separating two ferromagnetic grains (including vacuum) [2-4] could not explain inter-grain magneto-resistance in half-metals. Polycrystalline and cold-pressed Sr_2FeMoO_6 (SFMO) samples with identical metallic thermopower (bulk properties) exhibited very different zero-field and magneto-conductance [5]; it was proposed that this difference is due to different magnetic properties of the grain-boundaries. The magneto-resistive behaviour of $(BaSr)_2FeMoO_6$ [6] was explained in terms of tunnelling between two correlated spin glass-like surfaces separated by a thin insulating layer. The magnetization and magneto-resistance (MR) data for a series of SFMO samples [7] were interpreted in terms of a model in which the grain-boundary regions act as spin valves; this MR was termed SVMR. It was shown [8] that SVMR is a generic feature of the metallic, ferromagnetic double-perovskite family as a whole. Careful ac susceptibility measurements on a highly ordered polycrystalline sample of SFMO [9] were able to separate the barrier layer signal from the bulk. The presence of an intrinsic insulating boundary layer, about 2 unit cells thick, around grains of $(LaSr)MnO_3$ with magnetic properties different from those of the bulk [10], is held responsible for the depressed magneto-transport properties in manganite based magnetic junctions.

Unlike the difficulty in separating the magnetic properties of the layers from those of the bulk [9], it is relatively easy to study the electronic properties of the grain skin layers when the electronic transport is dominated by inter-grain tunnelling as is the case in most of the polycrystalline samples of the title materials. In this report we focus on the zero-field conductivity of various samples of the five title compounds using results accumulated in this lab. Some of the unpublished results will be presented for the first time here. This comparative study revealed some important features of the grain-boundaries of these half-metals.

2.1 Inter-grain tunnelling in $Sr_2BB'O_6$

Table I shows the five title double-perovskites (with abbreviations), their ionic configuration, nominal (ideal) saturation magnetization (M_i) and T_c. While the bulk of these materials is metallic, as confirmed by their metallic-like thermopower [12], the zero-field conductivities (σ(T)) of polycrystalline samples are non-metallic (the conductivity increases with increasing T). Metallic-like resistivity was found in a single crystal of SFMO [13]. The inter-grain tunnelling conductivity depends strongly on preparation conditions and often exhibits unusual T-dependence. The most remarkable behaviours are the linear-in-T conductivities from liquid He temperatures up to RT, for *all* our sintered and granular samples of SFMO, irrespective of preparation conditions, for some samples of SFRO and of SCMO, and the linear-in-T^2

[a] phr06bf@physics.technion.ac.il`

conductivity over the same range of T, for some samples of SCMO [14].

Table 1. The five $Sr_2BB'O_6$

$Sr_2BB'O_6$	Ionic configuration	M_i (μ_B/f.u.)	T_c (K)
Sr_2FeMoO_6 (SFMO)	$Fe^{3+}(3d^5)Mo^{5+}(4d^1)$	4	420
Sr_2FeReO_6 (SFRO)	$Fe^{3+}(3d^5)Re^{5+}(5d^2)$	3	400
Sr_2CrMoO_6 (SCMO)	$Cr^{3+}(3d^3)Mo^{5+}(4d^1)$	2	450
Sr_2CrWO_6 (SCWO) [11]	$Cr^{3+}(3d^2)W^{5+}(5d^1)$	2	390
Sr_2CrReO_6 (SCRO)	$Cr^{3+}(3d^3)Re^{5+}(4d^2)$	1	635

The temperature dependence of the conductivity for all our samples, except for porous SCRO, can be derived from the "fluctuation induced tunnelling" (FIT) model [15]. This model applies to metallic grains embedded in an insulating medium. Tunnelling occurs across small gaps (width w and area A) between large metallic grains; the small gaps are subject to large thermal fluctuations of the voltage. σ(T) predicted by this model is:

$$\sigma = \sigma_o e^{-\frac{T_1}{T_o+T}} = \sigma(0) e^{\frac{T_1}{T_o}\frac{T}{T_o+T}} \qquad (1)$$

where $k_B T_1 = (2/\pi)(A/w)(V_o/e)^2$ is the electrostatic energy within a parabolic potential barrier of width w and height V_o of a junction of area A; $T_1/T_o = \pi\chi w/2$ is the tunnelling constant where $\chi = \sqrt{(2mV_o/(h/2\pi)^2)}$, σ_o is a pre-exponent that may be regarded as independent of temperature and $\sigma(0)=\sigma_o \exp(-T_1/T_o)$. The FIT equation for σ(T) is an extension of the formula derived for a single junction to a network of fluctuating tunnelling junctions [15]. For $T<<T_o$ Eq. (1) represents elastic tunnelling and for $T>>T_o$ - activated conductivity with activation energy $k_B T_1$. The effect of the thermal fluctuations is to reduce the barrier's height and width; for $T=T_o$ the effective tunnelling constant is half its value at $T=0$. This equation includes the unusual and interesting cases mentioned above for specific ranges of the parameter T_1/T_o and of T/T_o. In Ref. [14] we showed that for $T_1/T_o < 3$ a linear function of T fits σ(T) over a T/T_o range that increases with T_1/T_o. The correlation parameter of the linear fit to Eq. (1) for $T_1/T_o \leq 3$ and $T/T_o \leq 1.1$ is $R^2=0.9999$. In this range, σ(T) varies up to a factor of 5, in good agreement with our findings (see figure 4 in Ref. [14]). We showed also that $(\sigma(T)-\sigma(0)) \propto T^2$ ($R^2=0.9999$), for a narrow range of T_1/T_o around 8 and T/T_o up to ~ 1.8. Within this range $\sigma(T)$ may vary by more than two orders of magnitude, again in good agreement with our findings (see figure 3 in Ref. [12]).

All SFMO samples exhibit linear $\sigma(T)$. In other compounds conductivity linear-in-T or linear-in-T^2 (over a wide temperature range) are special cases. However, except for SCRO, $\sigma(T)$ for all sintered samples obeys the FIT model with parameters within a wide range that depend on the preparation conditions. Our sintered SCRO samples were porous and their conductivity over an unprecedented wide range of T was of Berthelot-type ($\ln(\sigma(T)/\sigma(0)) = T/T_B$ where T_B is a constant of the order of a few tens of K) [16]. This behaviour can be derived from Tredgold's "vibrating barrier tunnelling" model [17]. Eq. (1) can be reduced to a Berthelot-type formula for $T_1/T_o >> 1$ and $T/T_o << 1$ with $T_B = T_o^2/T_1$ but then the values of the fitting parameters to our data become non-physical. Interestingly, σ(T) for cold-pressed (c.p.) SCRO obeys the FIT model with reasonable parameters (see below).

The FIT model has been extended to electric-field dependent conductivities The nonlinear I-V characteristics measured on some SFMO samples (using pulsed currents in order to avoid Joule heating) are consistent with the extended FIT model, at least qualitatively [18].

The FIT model does not address magnetic interactions. Since it was applied successfully to at least three groups of magnetic materials (our title materials, CrO_2 and its composites [19, 20] and Co-based nanocomposites [21]), it may be assumed that the influence of the magnetic interactions affect the nature of the tunnelling barrier and the pre-exponent. As M_i of our samples varies between 1 and 4, we attempted to detect correlations between the tunnelling parameters of the exponent of Eq. (1) and M_i.

2.2 Experimental results and discussion

Table 2 contains the fitting parameters of Eq. (1) to the experimental σ(T): σ(0), T_1, T_o and T_1/T_o, for our samples of $Sr_2BB'O_6$. The labels of the five groups of samples and data sources (references to our previous publications and figures 1 and 2 shown here), are followed by the fitting parameters. Only two parameters in the exponent are independent, but for convenience all three are shown (T_1, T_o and T_1/T_o). We also show the fitted parameters for a cold-pressed $Sr_{1.5}La_{0.5}FeMoO_6$ (LSFMO). Additional plots of σ(T) for SFMO are shown in Ref. [18]; all are straight lines up to RT. The slopes of the plots for the cold-pressed samples are steeper than those for the sintered samples. The conductivities of the samples at T=0 (σ(0)), spread over many orders of magnitude, from 10^{-6} to 10^{2} $(\Omega cm)^{-1}$. The highest σ(0), (=74.5 $(\Omega cm)^{-1}$, for sample SFMO(N1)) is about 50 times lower than the metallic conductivity of an SFMO single crystal at T=0 [13].

The upper curve in figure 1(a) shows σ(T) of a sintered SFRO sample that underwent a short heat treatment at 500°C in Ar5%H_2. The maximum indicates mixed grain-boundary and metallic conductivity. A similar behaviour is seen in Figure 2 of Ref. [22] for an SFRO sample sintered in an Ar atmosphere. Prolonged heat treatment of

Table 2. Fitting parameters for Eq. (1), for $Sr_2BB'O_6$ polycrystalline samples

Sample, figure, [Ref.]	σ(0) $(\Omega cm)^{-1}$	T_1 (K)	T_o (K)	T_1/T_o
SFMO(N1) 2, [18]	74.5	5171	2478	2.09
SFMO(r) 4, [14]	33.8	6989	2551	2.74
SFMO(c.p.) 2, [14]	0.72	1586	582	2.73
SFRO(Ox) 1(a), here	2.50	396	494	0.80
SFRO(S1) 1(b), here	3.88	1117	703	1.59
SFRO(S2) 1(b), here	13.0	276	397	0.70
SFRO(c.p.) 1(b), here	0.19	8111	1329	6.10
SCMO(A) 2(a), [14]	1.02	712	263	2.71
SCMO(C) 2(a), [14]	2.48	455	117	3.89
SCMO(E) 2(a), [14]	6.10	390	130	3.00
SCMO(A+Ox) 2(a), [14]	4.6×10^{-4}	1104	207	5.33
SCMO(D) 2(b), [14]	0.31	1405	228	6.16
SCMO(B1) 3(b), [14]	6.3×10^{-4}	1430	180	7.94
SCMO(B2) 3(b), [14]	5.6×10^{-4}	1177	152	7.74
SCWO 6(a) [11]	0.045	260	118	2.20
SCWO 6(a) [11]	0.030	461	213	2.16
SCWO(c.p.) 2, here	2×10^{-6}	1850	200	9.25
SCRO(c.p.) 2, here	1.2×10^{-4}	4071	383	10.63
LSFMO(c.p). 4, [14]	0.47	941	298	3.16

r-reduced, c.p.-cold-pressed, Ox – oxidized

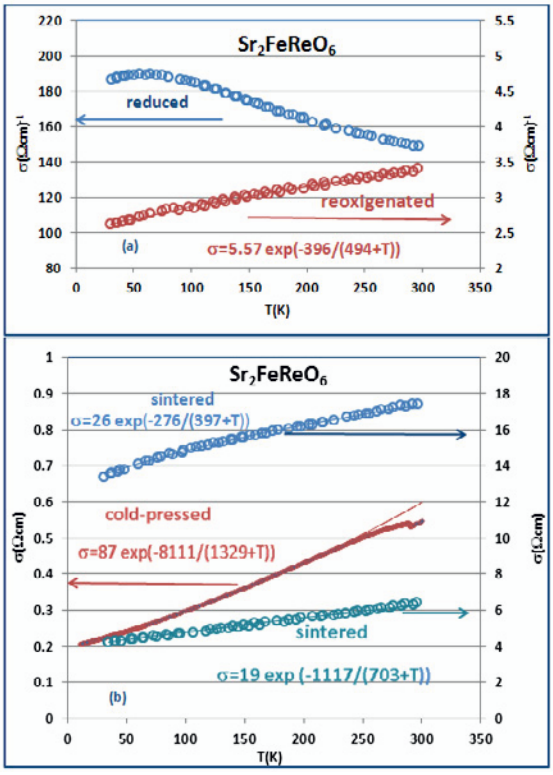

Fig. 1. Conductivity versus temperature of (a) a sintered sample of Sr_2FeReO_6 heat treated at 500° C in a reducing atmosphere (upper curve) and later re-oxygenated at 400°C (lower curve), and (b) two additional sintered samples and one cold pressed sample. Solid lines in (a) and (b) represent Eq. (1) fitted to experimental data.

our sample in air at 400°C restored inter-grain tunnelling and the σ(T) plot straightened up (see lower curve in Fig. 1(a)). Figure 1(b) shows three more plots of σ(T) for SFRO samples, including one for a c.p. sample. The data for the c.p. sample exhibit unusual behaviour at high temperatures and Eq. (1) could be fitted only up to 250 K.

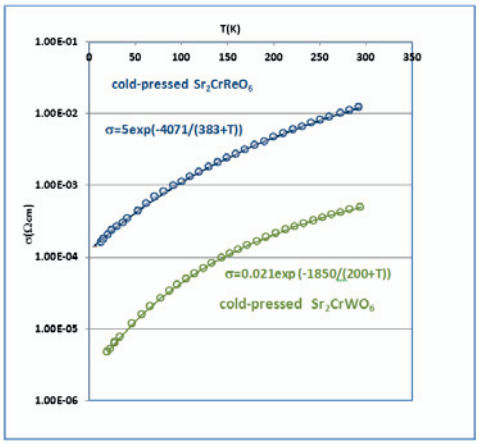

Fig. 2. Conductivity versus T of cold-pressed samples of $SrCr_2WO_6$ (lower curve) and Sr_2CrReO_6 (upper curve). Solid lines represent Eq. (1) fitted to experimental data.

Figure 2 presents plots of $\sigma(T)$ for c.p. samples of SCWO and SCRO that were not included in the previous reports [11, 16]. Although the conductivities of porous SCRO samples are of Berthelot type, figure 2 shows that Eq. (1) fits $\sigma(T)$ of the c.p. sample.

The three parameters T_1, T_o and T_1/T_o are plotted versus M_i in figures 3(a)-(c). M_i for LSMO is 3.5. While no correlations are seen in figures 3(a) and (b), figure 3(c) exhibits two remarkable features:

1.The data of T_1/T_o (the tunnelling constant $\pi\chi w/2$) for SFMO fall between 2 and 3, irrespective of microstructure of the samples. Within the FIT model this corresponds to the remarkable linearity of σ(T). The independence from microstructure hints at the presence of an intrinsic insulating boundary layer through which tunnelling occurs, with well-defined electronic (and magnetic) structure. Note that the tunnelling constant depends only on the width w and the height V_o of the barrier. For a thickness w of the order of the c-axis lattice constant of SFMO (=7.92 Å) and the range of T_1/T_o given in Table II the values of V_o range between 0.25 to 0.5 eV, far higher than k_BT up to RT. This inequality is still valid for $w=2c$ but not for a much larger factor. As mentioned in the introduction, the thickness of the insulating boundary layer found in LSMO is about two unit cells, close to our estimate.

2. The data of T_1/T_o for cold pressed samples (*i.e.* for bare boundaries) lie close to a straight line that extrapolates to zero near M_i=5 which corresponds to vanishing minority spins (see Table I). The possibility that such a simple analytical function fits the dependence of $\pi\chi w/2$ on M_i for this set of half-metallic c.p. samples requires further experimental and theoretical support. Since the variation in the lattice parameters in this family of compounds is negligible, the steep increase in the

value of T_1/T_o with decreasing M_i may be due to the increase of the thickness of the insulating layer, leaving V_o comparable with that of SFMO.

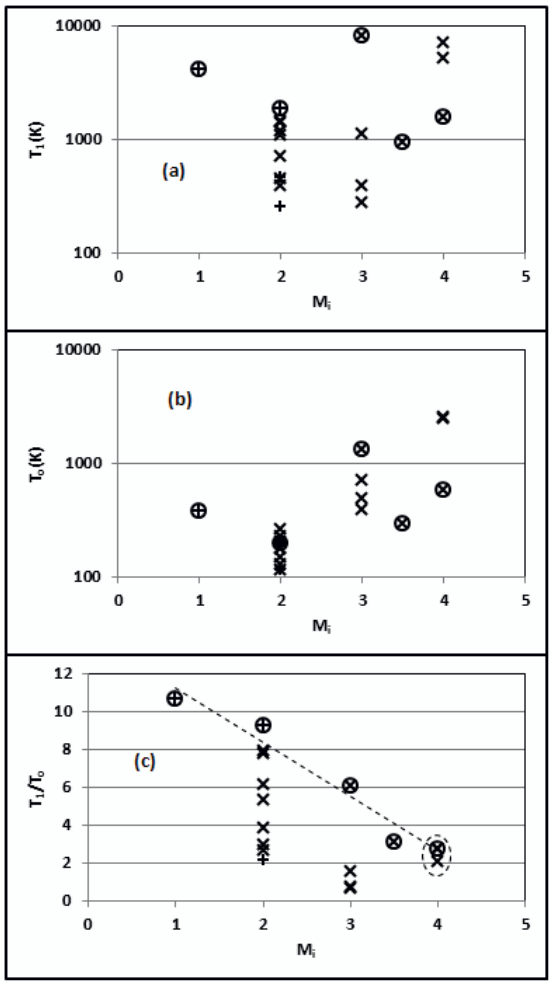

Fig. 3. Fitting parameters T_1, T_o and the tunnelling constant - T_1/T_o as function of M_i. For M_i=2 the symbol × represents samples of SCMO and + the samples of SCWO. Encircled symbols represent data for cold pressed samples. Note that for all SFMO samples, T_1/T_o falls between 2 and 2.75 (within the range of linear σ(T)). The values of T_1/T_o for the cold pressed samples increase almost linearly with M_i.

Eq. (1) shows that the higher T_o (relative to RT), the closer is inter-grain tunnelling to elastic tunnelling. Table II and figure 3(b) show that, for only 3 samples out of 19, T_o > 1000 K, namely for two polycrystalline samples of SFMO (in figure 3(b) the two symbols coincide) and for one c.p. sample of SFRO. Note that for SFMO(N1) the ratio σ(T)/σ(0) is only 1.25. T_o (or T_1) depends on the area A of the typical junction while T_1/T_o is independent of A. In the case of SFMO the low values of T_o of the c.p. sample, as compared to those of of the sintered samples, are probably due to smaller A. This is qualitatively consistent with reduced σ(0).

The wide spread of the FIT parameters in Table II implies a broad range of magneto-conductance behaviors. Ref. [5] shows that for sintered SFMO samples the magneto-conductance is much higher than that for a c.p. sample at all temperatures. This requires a more systematic investigation.

References

1. D. Serrate, J. M. De Teresa and M R Ibarra, J. Phys. Condens. Matter **19**, 023201 (2007) and references therein
2. M. Julliere, Phys. Lett. **54A**, 225 (1975)
3. J. C. Slonczewski, Phys. Rev. B **39**, 6995 (1989)
4. J. Inoue and S. Maekawa, Phys. Rev. B **53**, R11927 (1996)
5. B. Fisher, K. B. Chashka, L. Patlagan and G. M. Reisner, J. Magn. Magn. Mater. **272-276**, 1790 (2004)
6. D. Serrate, J. M. De Teresa, P. A. Algarabel, M. R. Ibarra, and J. Galibert, Phys. Rev. B **71**, 104409 (2005)
7. D. D. Sarma, S. Ray, K. Tanaka, M. Kobayashi, A. Fujimori, P. Sanyal, H. R. Krishnamurthy, and C. Dasgupta, Phys. Rev. Lett. **98**, 157205 (2007)
8. S. Jana, S, Middey and S. Ray, J. Phys. Condens. Matter **22**, 346004 (2010)
9. S. Ray, S. Middey, S. Jana, A. Banerjee, P. Sanyal, R. Rawat, L. Gregorratti and D. D. Sarma, EPL **94**, 47007 (2011)
10. S. Valencia, L. Pena, Z. Konstantinovic, Ll. Balcells, R. Galceran, D. Schmitz, F. Sandiumenge, M. Casanove and B. Martinez, J. Phys. :Condens. Matter **26,** 166001 (2014)
11. Sr_2CrWO_6 has been confused in the past with $Sr_3Cr_2WO_9$, which has a much higher T_c. Preparation of these two distinct compounds as single phases was reported in: B. Fisher , K. B. Chashka, L. Patlagan, and G. M. Reisner,Phys. Rev. B **71**, 104428 (2005)
12. B. Fisher, J. Genossar, K. B. Chashka, L. Patlagan and G. M. Reisner, Curr. Appl. Phys. **7**, 151 (2007)
13. Y. Tomioka, T. Okuda, Y. Okimoto, R. Kumai, K. -I. Kobayashi and Y. Tokura, Phys. Rev. B **61**, 422 (2000)
14. B. Fisher, J. Genossar, K. B. Chashka, L. Patlagan, and G. M. Reisner, Solid State Commun. **137**, 641 (2006) and references therein
15. Ping Sheng, Phys. Rev. B **21**, 2180 (1980) and references therein
16. B. Fisher, K. B. Chashka, L. Patlagan, and G. M. Reisner, Phys. Rev. B **70**, 205109 (2004)
17. R. H. Tredgold, Proc. Phys. Soc. London **80**, 807 (1962)
18. B. Fisher, K. B. Chashka, L. Patlagan, and G. M. Reisner, Phys. Rev. B **68,** 134420 (2003)
19. A. Bajpai and A. K. Nigam, Phys. Rev. B **75**, 064403 (2007)
20. Fan Yin-Bo, Zhang Cai-Ping, Du Xiao-Bo, Wen Ge-Hui, Ma Hong-An and Jia Xiao-Peng, Chin. Phys. Lett. **30**, 037502 (2013)
21. T. Wen and K. M. Krishnan, J. Phys. D: Appl. Phys. **44**, 393001 (2011)
22. K.-I. Kobayashi, T. Kimura, Y. Tomioka, H. Sawada, K. Terakura and Y. Tokura, Phys. Rev. B **59**, 11159 (1999).